ChemComm

Needle Grass-like Cobalt Hydrogen Phosphate on Ni Foam as Effective and Stable Electrocatalysts for Oxygen Evolution Reaction

Journal:	*ChemComm*
Manuscript ID	CC-COM-05-2019-003929.R1
Article Type:	Communication

Chem Commun

COMMUNICATION

Needle Grass-like Cobalt Hydrogen Phosphate on Ni Foam as Effective and Stable Electrocatalysts for Oxygen Evolution Reaction

Received
Accepted

DOI: 10.1039/

www.rsc.org/

Zemin Sun,# Mengwei Yuan,# Liu Lin, Han Yang, Huifeng Li, Genban Sun,* Xiaojing Yang, Shulan Ma

Exploring an efficient non-precious metal electrocatalysts for oxygen evolution reaction (OER) is a challenging task in sustainable energy systems. Herein, a facile and novel three dimensional (3D) needle grass-like $CoHPO_4 \cdot H_2O$ on Ni foam (CoHPO/NF) has been prepared as effective and robust OER electrocatalysts for the first time. The unique 3D topological structure of CoHPO benefits to expose more electrocatalytic active sites and facilitate the mass transport. The coordination HPO_4^{2-} anions work as OH^- trap to synergistically enhance the process of OER. Because of these advantages, it exhibits an extraordinary OER performance with a low overpotential of only 350 mV at 50 mA cm^{-2}. Notably, it also owns excellent long-term stability. According to the theory calculation, the electron structure of the Co was significantly influenced by the coupled HPO_4^{2-} species, which leads to the superior activity for OER. All the findings imply CoHPO/NF would be a promising material to substitute for noble metals in overall water splitting.

Since the first industrial revolutions, the utilization of fossil fuels has brought great convenience to modern society. However, the fossil energy's massive mining and utilization have caused the serious air pollution and the ecological environment destruction.[1-2] Hydrogen as a new, powerful and clean fuel source has attracted great attention recently all over the world.[3] Nearly three-fourths of the earth is ocean. Water electrolysis through using renewable energy such as solar and wind energy would be the most promising method.[4] Unfortunately, the sluggish kinetics for hydrogen evolution reaction (HER) and OER have severely restricted its practical development.[5,6] The OER process was four-proton-coupled electron transfer steps, while HER is only two electron reaction. [7-9] Thus, the process of OER requires more energy to overcome the kinetic barrier. It is necessary to develop an effective OER electrocatalyst to enhance the water splitting reaction. Nowadays, Ru- and Ir-based catalysts are considered as the outstanding electrocatalysts for OER.[10] Both of them are noble metals, the high costs limit their practical application. Therefore, to develop durable, efficient and economical oxygen evolution catalyst is highly urgent.

Numerous studies have been concentrated on exploring non-noble metal catalysts.[11,12] Earth-abundant cobalt-based materials have been studied widely attentions for OER, because of its unique electronic characteristics and low-cost.[13-15] Compared with traditional Co-based catalysts, such as metal oxides, hydroxides, phosphides and sulfides, there were few studies for $CoHPO_4$ materials in this subject.[16-20] However, for $CoHPO_4$ materials, the coordination HPO_4^{2-} anions could work as OH^- trap due to the Lewis acid properties, it can effectively strengthen the OH^--absorption capacity. When the OH^-'s concentration increased near catalysts, it might synergistically enhance the OER performance to decrease the over-potential. As a result, utilizing this synthetic strategy, developing a facile and producible strategy to prepare an effective and robust $CoHPO_4$ catalyst might own excellent catalytic activity in alkaline media.

In this work, a novel, robust and alkali resistance needle grass-like $CoHPO_4 \cdot H_2O$ (CoHPO) on Ni Foam was synthesized *via* one-pot hydrothermal method. The change of CoHPO morphology on Ni Foam was similar to the growth of grass. With the hydrothermal time prolonging, the CoHPO was from scanty (**Figure 1a**) to abundant (**Figure 1b**) and then needle grass lawn grew on Ni foam uniformly (**Figure 1c**). According to the result of SEM, it showed that the CoHPO was needle grass-like shaped with uniform length. According to the TEM image of CoHPO in **Figure 1d**, it also can be seen that it was needle-shaped with a length size of *ca.* 3 μm and an average diameter of *ca.* 160 nm. Moreover, **the insert of Figure 1d** showed the corresponding selective area electron diffraction (SAED) pattern with one set of diffraction spots, which revealed the single crystalline nature and high quality crystallization for CoHPO. The 3D topological structure could facilitate diffusion of electrolyte and gas to enhance OER performance. The lattice fringes was shown in **Figure 1e**, the interplanar spacing of CoHPO was 0.80 nm with well parallelism, corresponding to the (110) plane of CoHPO. The elemental mapping has been conducted to further verify the surface

Beijing Key Laboratory of Energy Conversion and Storage Materials, College of Chemistry, Beijing Normal University, Beijing 100875, China
* E-mail: gbsun@bnu.edu.cn;
Electronic Supplementary Information (ESI) available: SEM, polarization curves, AC impedance spectra,etc See DOI:

elements of CoHPO in **Figure 1f**, and the Co, O, and P were uniformly distributed on the surface of nano-needle.

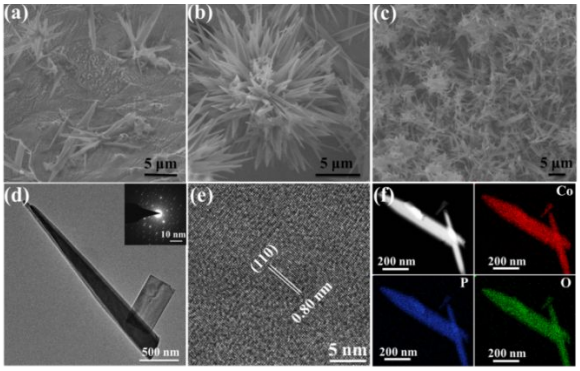

Figure 1. SEM of CoHPO/NF with hydrothermal reaction for 6 h (a), 9 h (b) and 12 h (c). TEM (the inset is SAED) (d), HRTEM (e) and elements mapping (f) of CoHPO obtained after 12 h.

To investigate the crystallographic phases of as-prepared electrocatalysts, the X-ray powder diffraction (XRD) patterns were measured (**Figure 2a)**. The XRD of the CoHPO powder matched well with the standard patterns (JCPDS no. 45-0373), which suggested the formation of CoHPO. The XRD pattern of CoHPO/NF was also collected (**Figure S1)**. It can be observed that the CoHPO was successfully grown on the Ni Foam, which was in accord with the result of SEM. Without $K_2HPO_4{\cdot}3H_2O$ added, the powder product was $Co(OH)_2$, in accordance with JCPDS 45-0031. The XRD pattern of $Co(OH)_2$/NF (Figure S1) showed the clear diffraction peaks of $Co(OH)_2$, which indicated that it was successfully grown on Ni Foam. According to the SEM of $Co(OH)_2$/NF, it also can be seen abundant needle grass-like $Co(OH)_2$ were grown on Ni foam in Figure **S2a**, **From Figure S2b,** it clearly indicated that $Co(OH)_2$ and CoHPO were in similar morphology. In addition, the loading of CoHPO and $Co(OH)_2$ on Ni Foam was analyzed through ICP-MS, which listed in **Table S1**. The loading of CoHPO and $Co(OH)_2$ was *ca.* 0.35 and 0.38 mg cm^{-2}, respectively. In **Figure 2b**, the peak centered at 483 cm^{-1} both in CoHPO and $Co(OH)_2$, which represented the ν(Co–O) stretching vibrations. Compared with $Co(OH)_2$, the peaks appeared at 781 cm^{-1} and 1153 cm^{-1}, which were assigned to P-O-H group. [21, 22] Besides, the peaks at 1035 cm^{-1} demenstrated P-O-Co stretching vibrations, which demonstrated that the existence of CoHPO. [21] The surface chemical states and elemental valences were studied *via* XPS. The elements of Co, P, and O were detected in survey spectrum (**Figure 2c**). As shown in **Figure 2d**, the Co $2p_{3/2}$ branch could be further divided into two peaks at 782.8 and 781.0 eV, corresponding to the bond of Co^{2+} and Co^{3+}. [23] For the Co $2p_{1/2}$ also presented two sharp peaks at 798.1 and 797.0 eV, which also indicated the existence of Co^{2+} and Co^{3+}. There were two satellites at 786.4 and 803.1 eV, which were attributed to the shake-up excitation of Co^{2+}.[24] According to the XPS spectrum of P 2p in **Figure 2e**, it displayed two peaks at 132.7 and 133.4 eV, which belonged to the 2p3/2 and 2p1/2 in phosphate groups.[25] Besides, the O 1s was also measured in **Figure 2f**, in which peaks at 530.0, 530.4 and 532.1 eV were corresponding to Co-O-P, P-O-H and H_2O, respectively.[26] The structure data and valence state information can further prove that CoHPO has been synthesized *via* one-pot hydrothermal method.

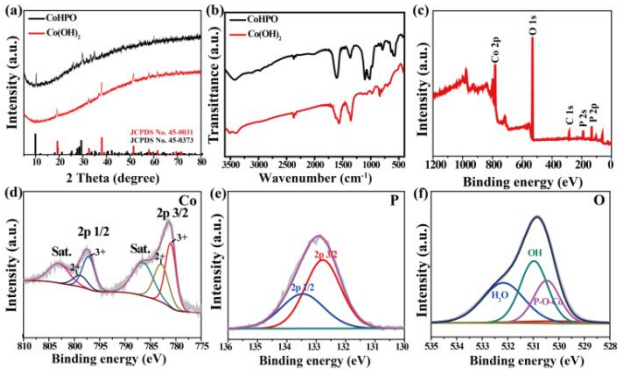

Figure 2. XRD (a) and IR spectra (b) for CoHPO and $Co(OH)_2$, XPS survey spectrum (c) of CoHPO, high-resolution peak-fitting XPS spectra of Co 2p (d), p 2p (e) and O 1s (f).

Electrochemical OER activities of the CoHPO/NF and $Co(OH)_2$/NF have been investigated in 1 M KOH solution with O_2-saturated. **Figure 3a and 3b** illustrated the results of LSV. When the current density reached to 50 mA cm^{-2}, it required an overpotential of 557 mV for Ni foam, indicating Ni Foam was almost no catalytic activity. Compared with Ni foam, the CoHPO/NF revealed excellent catalytic activities with an ultralow overpotential of 350 mV @ 50 mA cm^{-2}, much better than that of $Co(OH)_2$/NF, which was 437 mV @ 50 mA cm^{-2}. Notably, the performance of CoHPO/NF was also better than noble metal RuO_2-NF (373 mV @ 50 mA cm^{-2}). Furthermore, it possessed a low overpotential at high current density, implying that it had the potential of practical application. As for a higher current density 100 mA cm^{-2}, the overpotential of CoHPO/NF only 396 mV was required, much less than that of $Co(OH)_2$/NF (510 mV) and RuO_2-NF (438 mV). The performance of CoHPO/NF was also better than previous reported Co-based catalysts cited in **Table S2**. Besides, in order to confirm the catalytic performance of CoHPO, the same mass CoHPO powders were adhered by Nafion in the same area Ni foam (CoHPO-NF) to measure the OER activity in **Figure S3**. According to the LSV, it can be seen that the performance of CoHPO-NF was slightly lower than that of CoHPO/NF, but still better than that of $Co(OH)_2$/NF. The reason CoHPO/NF does well is that the CoHPO/NF had a stronger binding force between the catalysts and NF, compared with CoHPO-NF, the in-situ growth CoHPO/NF possessed faster mass transfer properties, more excellent conductivity and mechanical robustness to enhance enhanced the OER kinetics. Furthermore, the CoHPO in-situ growth on carbon paper (CoHPO/CP) also has been prepared. It also showed well performance which was very near that of CoHPO/NF, better than that of CoHPO-NF. All of them demonstrated that the CoHPO owned well OER activity.

The Tafel slope was an important assessment for reaction kinetics of the catalysts. The Tafel slope of CoHPO (**Figure 3c**) was only 113 mV dec^{-1}, lower than that of $Co(OH)_2$ and Ni foam with 126 and 174 mV dec^{-1}, which indicated the well reaction kinetics. Besides, the OER kinetics was very close to RuO_2-NF (125 mV dec^{-1}). To further study electrode reaction kinetics of CoHPO, EIS data was

collected at 1.55 V vs. RHE in **Fugure 3d.** The Nyquist semicircle of the CoHPO/NF electrode was much lower than that of $Co(OH)_2$/NF and Nickel foam, indicating the lower charge transfer impedance and the faster reaction kinetics for CoHPO/NF. The results of Tafel slope and EIS demonstrated that CoHPO owned a faster electron transport performance in OER process. The electrochemical double-layer capacitance (Cdl) could reflect the electrochemically active surface area, which was proportional to the amount of catalytic active sites. The CV curves at different scanning rates (**Figure S4a** and **S4b)** were collected to calculate the Cdl. As shown in **Figure 3e**, the Cdl of CoHPO was 100 mF cm^{-2}, which was ten times more than that of the $Co(OH)_2$ catalyst. It can be ascribed that the HPO_4^{2-} had better ability to capture OH^- coordination, compared with $Co(OH)_2$, which would benefit to enhance OER activity.

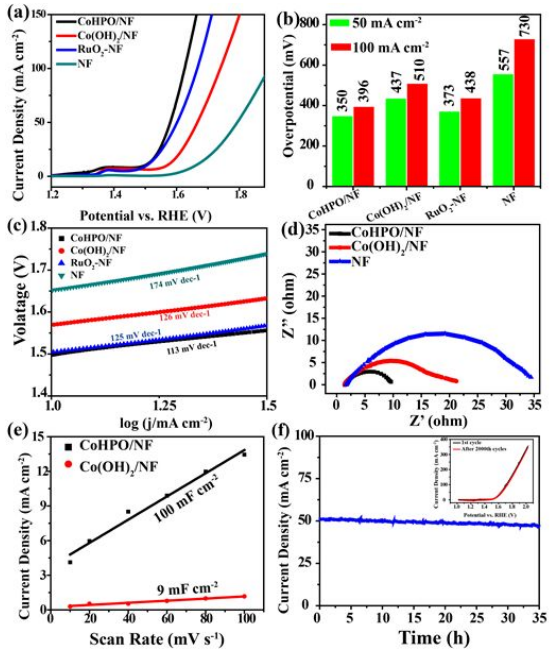

Figure 3 Polarization curves (a), the overpotential at 50 and 100 mA cm^{-2} (b) and Tafel plots (c) of CoHPO/NF, $Co(OH)_2$/NF, RuO_2-NF and NF. (d) Nyquist plots of CoHPO/NF, $Co(OH)_2$/NF and NF. (e) Estimation of Cdl by plotting the current density variation. (f) the long-term durability tests at 1.60 V in a 1.0 M KOH electrolyte, The inset of Figure 3f shows Stability of CoHPO/NF with an initial polarization curve and after 2000 cycles in 1.0 M KOH.

In addition, the reaction stability of the catalyst was one of the important marks for evaluating the quality of catalysts. Continuous CV measurement was carried out to assess the stability of the catalyst. The initial and final LSV curves were shown in the inset of **Figure 3f**. Even after 2000 cycles, the electrode performance was extremely stable and the loss is negligible. In addition, it remained a stable operation at 1.60 V with minimal current change in **Figure 3f**. The results demonstrated that the catalyst was superior in long-term electrochemical durability at high current density, only a mere 5.1 % decay after 35 h continuous electrolysis. After 35h electrolysis, the loading of CoHPO barely changed listed in **Table S3**, which demonstrated that the CoHPO owned well-stability in basic media. The XPS (**Figure S5**) and TEM (**Figure S6a**) for CoHPO after the long-time chronopotentiometric measurement revealed that the chemical state and needle-like morphology can still keep well after the OER catalysis. However, it can be observed from the TEM in **Figure S6b** that there was an amorphous film formed on surface of CoHPO, which may cover the reaction interface and lead to the slightly reduced electrocatalytic activity.

To further investigate the reason of the high reaction activity of the CoHPO in OER, the DFT was employed to theoretically analyze the electron structure of electrocatalysts.[27-31] The Total density of states (TDOS) of CoHPO and $Co(OH)_2$ presented an obvious electronic structure difference in **Figure 4a**. Compared with the $Co(OH)_2$, the higher TDOS in CoHPO suggested that it had the high activity of electrons, which could be more active to given or accepted in reactions along the pathway of the electrocatalytic reaction in **Figure 4a**. This result was consistent with that the high Cdl value of the CoHPO, which confirmed the CoHPO with higher activity in OER process. In Co-based electrocatalyst, the Co was the active site and its electron structure was the origin to determine the electrocatalytic performance. The partial density of states (PDOS) was calculated on the basis of electron structure, the bonding energy and the dominating valence-electron states for different atoms, d states of Co and p states of O atoms, were illustrated in **Figure 4b** and **4c**. It can be observed that the d state of Co was the main contribution, and the electron structure of the Co was significantly influenced by the coupled functional group, HPO_4 species, leading to the superior electron activity. The optimized structure of CoHPO and the corresponding valence electron localization function (ELF) isosurface were also calculated to study charge accumulation in the bonding region in **Figure 4d and S7.** Compared with 2D $Co(OH)_2$, the three dimensional CoHPO exhibited a wide range of space charge distribution of Co-centre in the crystal structure, suggesting more effective sites for electrocatalytic activity. Based on these results, the CoHPO was the high-performance electrocatalyst with unique electron structure and more active sties.

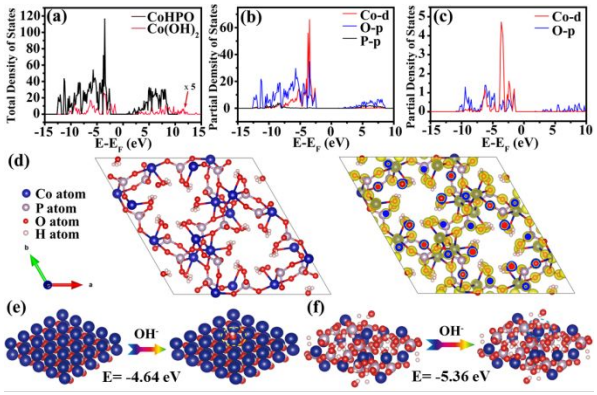

Figure 4 Total density of states for CoHPO and $Co(OH)_2$ (a). Partial density of states for different elements in CoHPO (b) and $Co(OH)_2$ (c). The crystal structures of the CoHPO and corresponding structure with ELF isosurfaces (d). Atomic models of (e) $Co(OH)_2$ and (e) CoHPO for DFT calculation. The adsorbed OH group at active sites was highlighted with the red circles.

Furthermore, except the unique electron structure of CoHPO, another important reason would be surface OH^- adsorption capability strengthened *via* coordination HPO_4^{2-} anions. Firstly, the same weight CoHPO and $Co(OH)_2$ powder put into the same volume concentration alkaline solution. According to **Figure S8,** compared with $Co(OH)_2$, the CoHPO can significantly lowered the pH value of the solution, which demonstrated that CoHPO can effectively enhance the surface OH^- adsorption capacity because of Lewis acid–base reaction. In addition, in order to further study the active centre, the Gibbs adsorption energy of OH* was an important influential factor. According to the DFT calculation in **Figure 4e-f**, the Cobalt centre of CoHPO showed stronger adsorption for OH^- compared with $Co(OH)_2$. Based on experimental and theoretical calculations, CoHPO catalyst owned excellent structural and catalytic activity in harsh alkaline media.

In conclusion, we have synthesized novel 3D needle grass-like CoHPO on Ni Foam and investigated the oxygen evolution reaction activity for the first time. It showed extraordinary OER activity with an ultralow overpotential of 350 mV at 50 mA cm^{-2}. Even at 100 mA cm^{-2}, it only needed 397 mV. Besides, it owned excellent structural and catalytic activity stability in harsh alkaline media. After 35h continuous electrolysis, the loading of CoHPO barely changed and there were merely 5.1 % decay of current density.This work open an exciting new avenue to substitute for noble metals in overall water splitting.

This work was supported by the National Science Foundations of China (21771024, 51572031 and 21871028)

Conflicts of interests

[#]Zemin Sun and Mengwei Yuan are equally contribution. All authors have given approval to the final version of the manuscript. There are no conflicts to declare.

Notes and references

1. C. Tang, R. Zhang, W. Lu, Z. Wang, D. Liu, S. Hao, G. Du, A. M. Asiri and X. Sun, *Angew. Chem. Int. Ed.*, 2017, **56**, 842-846.
2. X. Wang, K. Maeda, A. Thomas, K. Takanabe, G. Xin, J. M. Carlsson, K. Domen and M. Antonietti, *Nat. Mater.*, 2009, **8**, 76-80.
3. R. Zhang, X. Ren, S. Hao, R. Ge, Z. Liu, A. M. Asiri, L. Chen, Q. Zhang and X. Sun, *J. Mater. Chem. A*, 2018, **6**, 1985-1990.
4. B. You and Y. Sun, *Acc. Chem. Res.*, 2018, **51**, 1571-1580.
5. T. Abe, K. Fukui, Y. Kawai, K. Nagai and H. Kato, *Chem. Commun.*, 2016, **52**, 7735-7737.
6. H. Yoshida, R. Yamada and T. Yoshida, *ChemSusChem*, 2019, **12**, 1958 – 1965.
7. Y. Yan, B. Y. Xia, X. Ge, Z. Liu, A. Fisher and X. Wang, *Chemistry*, 2015, **21**, 18062-18067.
8. Y. Yan, B. Y. Xia, B. Zhao and X. Wang, *J. Mater. Chem. A*, 2016, **4**, 17587-17603.
9. C. Zhu, S. Fu, D. Du and Y. Lin, *Chemistry*, 2016, **22**, 4000-4007.
10. Y. Lee, J. Suntivich, K. J. May, E. E. Perry and Y. Shao-Horn, *J. Phys. Chem. Lett.*, 2012, **3**, 399-404.
11. L. Lin, Z. Sun, M. Yuan, J. He, R. Long, H. Li, C. Nan, G. Sun and S. Ma, *J. Mater. Chem. A*, 2018, **6**, 8068-8077.
12. Z. Sun, Y. Wang, L. Lin, M. Yuan, H. Jiang, R. Long, S. Ge, C. Nan, H. Li, G. Sun and X. Yang, *Chem. Commun.*, 2019, **55**, 1334-1337.
13. Z. Sun, M. Yuan, H. Yang, L. Lin, H. Jiang, S. Ge, H. Li, G. Sun, S. Ma and X. Yang, *Inorg. Chem.*, 2019, **58**, 4014-4018.
14. W. Li, S. Watzele, H. A. El-Sayed, Y. Liang, G. Kieslich, A. S. Bandarenka, K. Rodewald, B. Rieger and R. A. Fischer, *J. Am. Chem. Soc.*, 2019, **141**, 5926-5933.
15. H. Wang, E.. Feng, Y. Liu and C. Zhang, *J. Mater. Chem. A*, 2019, **7**, 7777-7783.
16. X. Zheng, H. Quan, X. Li, H. He, Q. Ye, X. Xu and F. Wang, *Nanoscale*, 2016, **8**, 17055-17063.
17. D. Ding, K. Shen, X. Chen, H. Chen, J. Chen, T. Fan, R. Wu and Y. Li, *ACS Catal.*, 2018, **8**, 7879-7888.
18. H. F. Wang, C. Tang, B. Wang, B. Q. Li and Q. Zhang, *Adv. Mater.*, 2017, **29**, 1702327.
19. H. Wen, M. Cao, G. Sun, W. Xu, D. Wang, X. Zhang and C. Hu, *J. Phys. Chem. C* 2008*,* **112**, 15948-15955.
20. M. W. Kanan and D. G. Nocera, *Science*, 2008, **321**, 1072-1075.
21. Y. Zhang, J. Shi, Y. Hu, Z. Huang and L. Guo, *Catal. Sci. Technol.*, 2016, **6**, 8080-8088.
22. H. B. Ortíz-Oliveros, R. M. Flores-Espinosa, E. Ordoñez-Regil and S. M. Fernández-Valverde, *Chem. Eng. J.*, 2014, **236**, 398-405.
23. C.-Z. Yuan, Y.-F. Jiang, Z. Wang, X. Xie, Z.-K. Yang, A. B. Yousaf and A.-W. Xu, *J. Mater. Chem. A*, 2016, **4**, 8155-8160.
24. X. H. Hou, L. Chena, , H. Xu, Q. Zhang, C. Zhao, L. Xuan, Y. Jiang, Y. Yuan, *Electrochim. Acta*, 2016, **210**, 462-473.
25. Y. Li and C. Zhao, *ACS Catal.*, 2017, **7**, 2535-2541.
26. L. Xie, R. Zhang, L. Cui, D. Liu, S. Hao, Y. Ma, G. Du, A. M. Asiri and X. Sun, *Angew. Chem. Int. Ed.*, 2017, **56**, 1064-1068.
27. I. Roger and M. D. Symes, *J. Am. Chem. Soc.*, 2015, **137**, 13980-13988.
28. J. Sun, A. Ruzsinszky and J. P. Perdew, *Phys. Rev. Lett.*, 2015, **115**, 036402.
29. A. Chakraborty, M. Dixit, D. Aurbach and D. T. Major, *npj Comput. Mater.*, 2018, **4**, 60.
30. J. Tao, J. P. Perdew, V. N. Staroverov and G. E. Scuseria, *Phys. Rev. Lett.*, 2003, **91**, 146401.
31. G. Kresse and J. Furthmuller, *Comput. Mater. Sci.*, 1996, **6**, 15-50.

Table of Content

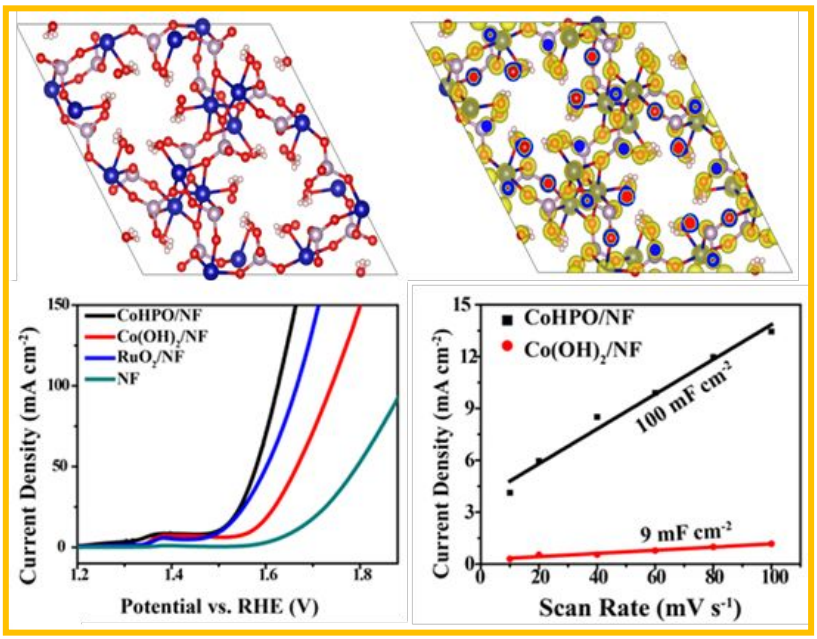

A novel three dimensional needle grass-like $CoHPO_4 \cdot H_2O$ on Ni foam has been prepared as effective and robust OER electrocatalysts.